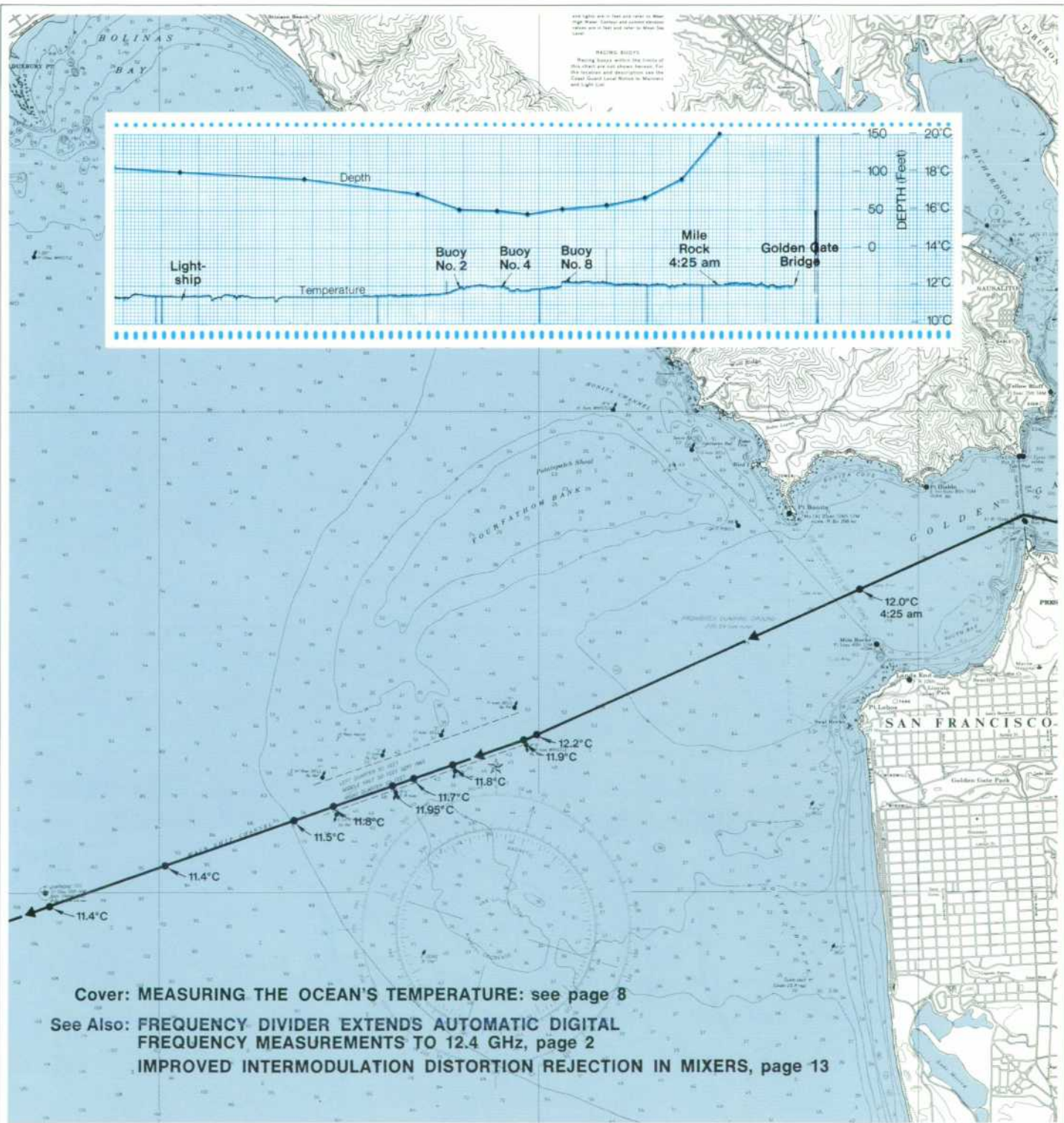


# HEWLETT-PACKARD JOURNAL



Cover: MEASURING THE OCEAN'S TEMPERATURE: see page 8

See Also: FREQUENCY DIVIDER EXTENDS AUTOMATIC DIGITAL FREQUENCY MEASUREMENTS TO 12.4 GHz, page 2

IMPROVED INTERMODULATION DISTORTION REJECTION IN MIXERS, page 13

# Frequency Divider Extends Automatic Digital Frequency Measurements to 12.4 GHz

*This sophisticated instrument lets an electronic counter measure microwave frequencies. The accuracy and simplicity of the counter are retained.*

WHEN THE ELECTRONIC COUNTER was introduced in the early 1950's, the major advantages it offered over existing techniques were simplicity and automatic operation. Tedious and complicated frequency measurements were suddenly reduced to utter simplicity. Soon, devices to extend the upper frequency limit of the counter became available. Unfortunately, they were not automatic and they were usually far from simple.

A new automatic frequency divider developed by *-hp-* successfully extends the frequency range of any electronic counter through X-band (12.4 GHz) while retaining the simple, automatic operation of the counter. Its basic principle of operation is that of a prescaler which divides the

input frequency by 100 or 1000. The reading on the counter requires only a decimal point shift for truly direct readout. The division ratio of 100 is used for frequencies below 1.2 GHz, and 1000 is used for frequencies above 1 GHz.

Fig. 1, showing the front panel of the instrument, attests to the simplicity of its operation. There is only *one* knob on the front panel — the one for selecting the division ratio. Once the division ratio has been chosen, the signal to be measured is applied at the input and the divided-down frequency appears at the output. A meter on the front panel indicates the approximate level (in dBm) of the input. The output, designed to drive a 50-ohm or higher load, features an automatic level control to maintain the output level at  $0 \text{ dBm} \pm 2 \text{ dBm}$  while the input varies over the specified range of  $-7 \text{ dBm}$  to  $+10 \text{ dBm}$ .

Because of its automatic operation, the new frequency divider is ideally suited for use by relatively unskilled personnel in production test areas, or for use as a component of a completely automatic, unattended system. Laboratories, too, will welcome the divider, because of the trend toward automated instruments which is now gaining momentum.<sup>1</sup>

## Operation

Although its front panel is the essence of simplicity, the new frequency divider is actually a highly sophisticated system. Its internal operation is quite unlike conventional frequency dividers. It has the fixed division



Fig. 1. Automatic Frequency Divider, *-hp-* Model 5260A, divides input frequencies between 0.3 GHz and 12.4 GHz by 100 or 1000 so they can be measured by a counter (counter shown is *-hp-* Model 5245L 50 MHz Counter). Divider operation is completely automatic except for selection of division ratio.

<sup>1</sup> For another example of the trend towards automatic instrumentation, read about the new microwave network analyzer in the February, 1967 issue of the 'Hewlett-Packard Journal.'

ratio of pulse-counting dividers, but demands a periodic input signal. It has frequency range capabilities similar to countdown dividers, but unlike these, it gives a constant division ratio. Unlike any other type of divider, it combines a constant division ratio with microwave frequency capability.

A simplified block diagram of this new type of frequency divider is shown in Fig. 2. The signal whose frequency is to be divided is sampled by two wideband feedthrough samplers in series.<sup>2</sup> The pulses which open the sampler gates to cause periodic samples to be taken are derived from two voltage-tuned oscillators (VTO's) operating at approximately 30 MHz. Each VTO drives one of the samplers. The output of the first sampler is returned to the tuning input of the first VTO via the necessary dc amplifiers and circuits to form an automatic phase-lock loop. When phase lock is established between the input frequency,  $f_x$ , and the VTO frequency,  $f_1$ , the two frequencies become harmonically related as shown in equation (1).

$$f_x = nf_1 \quad (1)$$

The frequency of the second VTO,  $f_2$ , tracks the frequency of the first VTO,  $f_1$ , with a slight offset. This offset results in a difference frequency at the output of the second sampler. This frequency,  $f_{out}$ , is  $n$ , the harmonic number, times the offset between the two VTO's. Thus,

$$f_{out} = n(f_1 - f_2) \quad (2)$$

If the offset is chosen to be  $f_1/100$  or  $f_1/1000$  the output frequency will be:

$$f_{out} = \frac{nf_1}{100} \quad \text{or} \quad \frac{nf_1}{1000} \quad (3)$$

Substitution of equation (1) into equation (3) yields the desired result.

$$f_{out} = \frac{f_x}{100} \quad \text{or} \quad \frac{f_x}{1000} \quad (4)$$

The technique used to maintain the offset between  $f_1$  and  $f_2$  is shown in Fig. 3. The voltage which tunes the first VTO is fed forward to the second VTO. Since these VTO's are nominally identical, they will be driven to nearly the same frequency. This constitutes a coarse control on the tracking of the two oscillators. Fine control is provided by a phase-lock loop which compares the difference frequency between the two oscillators with the frequency of the first oscillator divided by 100 or 1000.

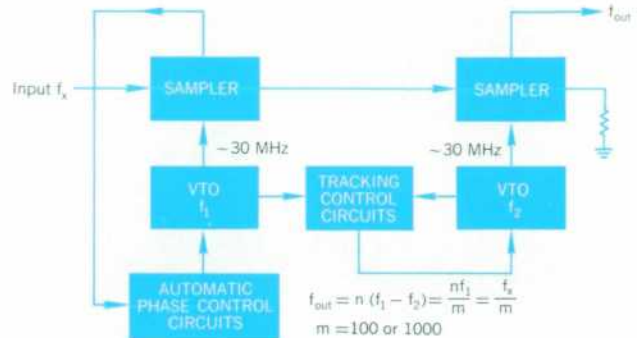


Fig. 2. Simplified block diagram of automatic frequency divider. Control circuits maintain indicated relationships between  $f_2$ ,  $f_1$ , and  $f_x$ .

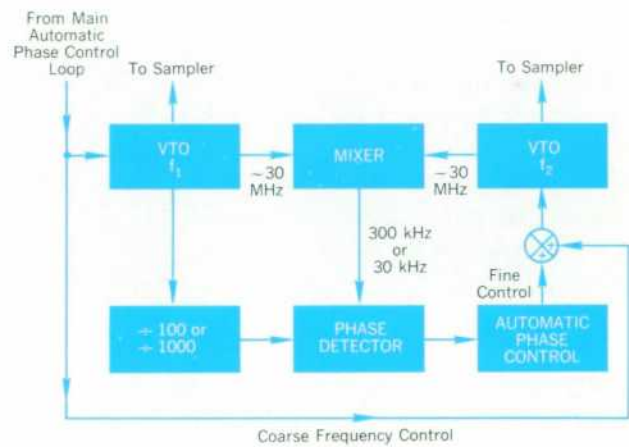


Fig. 3. Block diagram of tracking control used to keep frequency offset ( $f_1 - f_2$ ) equal to  $f_1/100$  or  $f_1/1000$ .

<sup>2</sup> These wideband samplers, developed by hp associates, are also used in a new -hp- microwave network analyzer and in a new -hp- sampling oscilloscope. For a description of the samplers, see W. M. Grove, 'A DC to 12.4 GHz Feedthrough Sampler for Oscilloscopes and other RF Systems,' *Hewlett-Packard Journal*, Vol. 18, No. 2, Oct., 1966. Another article in the same issue describes the new sampling oscilloscope: A. I. Best, D. L. Howard, and J. M. Umphrey, 'An Ultra-wideband Oscilloscope Based on an Advanced Sampling Device.' For a description of the network analyzer, see R. W. Anderson and O. T. Dennison, 'An Advanced New Network Analyzer for Sweep Measuring Amplitude and Phase from 0.1 to 12.4 GHz,' *Hewlett-Packard Journal*, Vol. 18, No. 6, Feb., 1967.

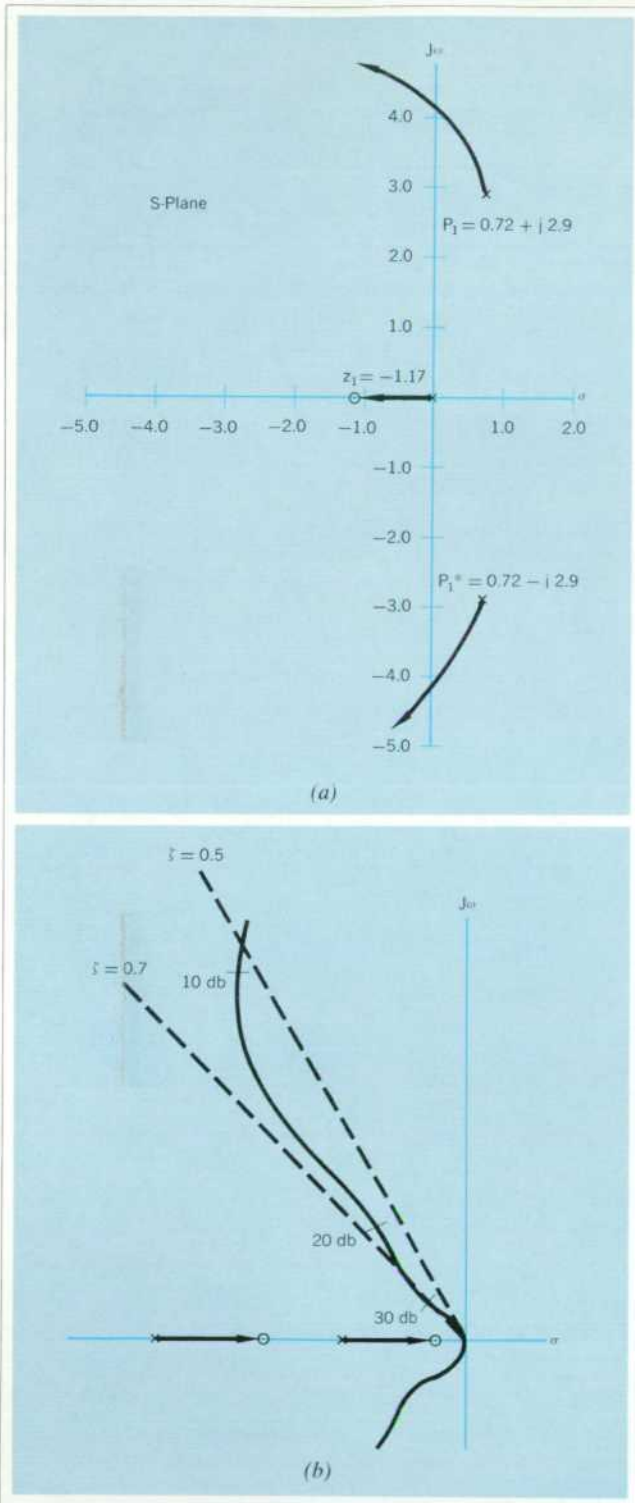


Fig. 4. (a). Magnified portion of root locus of main phase-lock loop. Note poles in right half plane which migrate to left half plane as loop gain increases. (b) Unmagnified root locus of main loop. Right-half-plane poles shown in (a) appear to start from origin on this plot. As loop gain increases by 30 dB, these poles move along line corresponding to damping ratios of 0.5 to 0.7. Thus loop is nearly critically damped over wide dynamic range.

A correction voltage from the phase detector is applied to the second VTO,  $f_2$ , through the necessary circuits to complete the phase-lock loop.

### Design Features

One of the major design features of the automatic frequency divider is the main phase lock loop, which enables the first VTO,  $f_1$ , to lock onto the input signal without any intermediate frequency in the loop. Until now, microwave phase lock loops have always used an intermediate frequency to establish the phase lock. This results in an offset between the microwave frequency and the harmonics of the VTO so that an exact harmonic relationship does not exist between  $f_x$  and  $f_1$ . The availability of the 12.4 GHz sampler has opened the door to zero-offset phase locking. Phase-related dc signals at a sufficiently high level to allow reliable phase locking are readily available from this sampler.

While the elimination of the intermediate frequency in the phase lock loop simplifies the system generally, one aspect becomes more complicated. In an IF system, input level variations are eliminated by the limiting action in the IF amplifier. With no IF, the amplitude information at the output of the phase detector (sampler) becomes indistinguishable from the phase information, and loop gain can be adversely affected. To overcome this difficulty, some means must be used for independently measuring the input signal amplitude and adjusting loop gain accordingly.

In the automatic frequency divider the input signal level is measured by detecting the level of the difference frequency out of the second sampler. The detected voltage is used to control the gain of the main phase lock loop. This same voltage is applied to the front panel meter to indicate the input signal level.

A disadvantage of previous microwave phase lock loops, which use harmonic mixers rather than samplers, has been the tendency of the harmonic mixer to generate harmonics of the input signal as well as harmonics of the local oscillator. The resulting phase locking between harmonics of the local oscillator and harmonics of the input signal caused a large amount of uncertainty in frequency measurements. The use of a wideband sampler instead of a harmonic mixer has eliminated this problem because the sampler does not generate harmonics of the input signal.

Two major requirements placed upon the main phase lock loop of the frequency divider by the requirement for automatic operation of the instrument are (1) an automatic search capability built into the loop to search out an input signal and lock onto it, and (2) a sufficiently wide gain margin for loop stability over a range of harmonic numbers ( $n$ ) from 10 to 400 (because loop gain is directly proportional to harmonic number).

# Frequency Divider + Integrated-Circuit Counter =12.4 GHz Digital Frequency Meter

Thanks to the space-saving habits of integrated circuits, *-hp-* engineers have managed to put an automatic frequency divider identical to the one described in the accompanying article *and* an eight-digit IC counter into one compact package. The combination measures any frequency between 0.3 GHz and 12.4 GHz, or between 10 Hz and 12.5 MHz, just like an ordinary counter. All the user has to do is connect the unknown signal to the proper input—there's one for 0.3 to 12.4 GHz and one for 10 Hz to 12.5 MHz—and select the proper frequency range. Everything else is automatic. The eight-digit readout includes the decimal point and measurement units. There is also a printer output (BCD is standard) with decimal point and units.

For measuring the high frequencies, the divider locks onto the input signal and supplies the IC counter with a signal which has 1/100 or 1/1000 of the input frequency. Both counter readout and printer printout are prevented until the



*-hp-* 5240A 12.4 GHz Digital Frequency Meter

frequency divider has locked onto the input signal. When low frequencies are being measured, the divider is bypassed and the IC counter measures the unknown frequency directly. (Incidentally, most of the IC's for the counter were produced in *-hp-*'s own IC facilities.)

Specifications for the 12.4 GHz Digital Frequency Meter are on p. 7.

The automatic search feature is achieved by inserting a low-frequency oscillator into the loop and adjusting the loop compensation so that the loop itself oscillates when loop gain is very low, and the low-frequency oscillator oscillates whenever the loop is open (unlocked). The oscillations sweep the first VTO through its frequency range until an input signal is found and phase lock is established.

A magnified portion of the root locus of the main phase lock loop is reproduced in Fig. 4(a). This shows the existence of poles in the right half plane which migrate to the left half plane as loop gain increases. The right-half-plane poles help to eliminate locking to spurious lower-level signals present along with the input signal. Since the loop is unstable for the low gain ensuing from a poor lock point it will automatically search out the best lock.

The locus of the poles as loop gain is increased still further as shown in Fig. 4(b). Here it can be seen that the poles move along a line maintaining a damping ratio of  $\zeta = 0.5$  to  $\zeta = 0.7$  as loop gain increases by 30 dB. Thus, with these poles dominating the system response, the loop is nearly critically damped over a very wide dynamic range.

## Performance

Overall performance of the automatic frequency divider can be judged by two factors. First, how well does it lock on to input signals with amplitude or frequency modulation? Second, how well can it produce a signal at

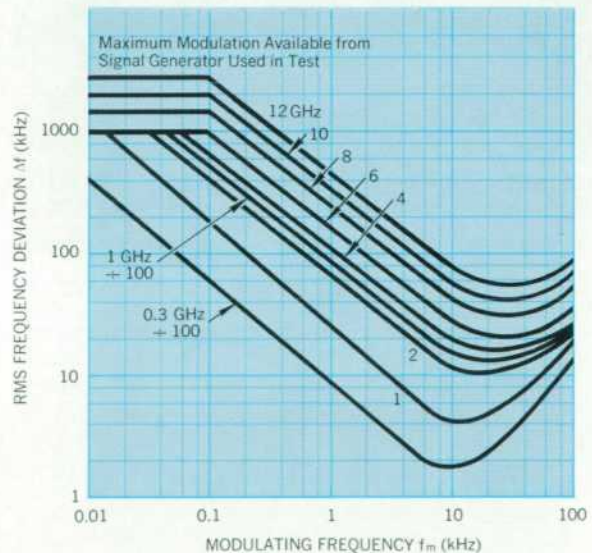


Fig. 5. Maximum frequency modulation on input signal that will permit frequency divider to lock on. These are typical measured characteristics at 0 dBm input. Division ratio was 1000 except where indicated.

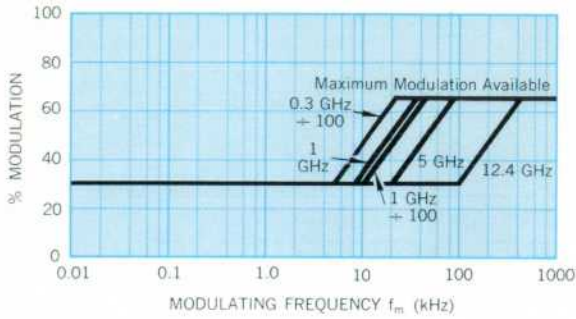


Fig. 6. Maximum amplitude modulation on input signal that will permit frequency divider to lock on. These are typical measured characteristics at 0 dBm input.

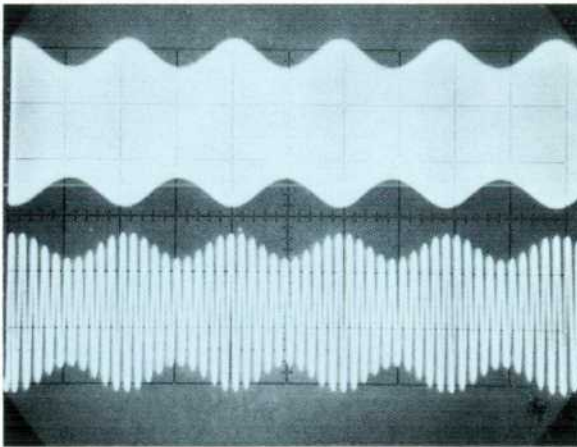


Fig. 7. For AM signals, frequency divider output tends to be a lower-frequency replica of the input. Traces show divider output for 1 GHz input signal, 20% amplitude modulated by 100 kHz signal. Top: divider output for division ratio  $m = 100$ . Bottom: divider output for  $m = 1000$ .

its output which is suitable to drive an electronic counter, even though the input signal may be amplitude or frequency modulated?

Fig. 5 is a plot of the maximum FM deviation and FM rate which can be tolerated by the main phase lock loop before it will fail to achieve phase lock. Each of the curves in Fig. 5 is an experimental curve for a single sinusoidal input signal, frequency modulated by a single sinusoidal signal of frequency  $f_m$ . (The rms frequency deviation  $\Delta f$  is proportional to the amplitude of the modulating signal.) These curves show, for example, that for an input frequency of 12 GHz and a modulating frequency of 1 kHz, the main loop will not achieve phase lock for rms frequency deviations greater than 480 kHz. However, when the modulating frequency is reduced to 100 Hz, the maximum allowable rms frequency deviation increases to 2.6 MHz.

If an input signal is frequency modulated by a non-sinusoidal signal, the frequency  $f_m$  and amplitude  $\Delta f$  of each component of the modulating signal must be taken into account. The effects of all components will be additive, so the performance of the frequency divider for each component will be degraded somewhat from that shown in Fig. 5. A detailed mathematical analysis of this problem is still in progress, so it is not yet possible to say precisely how the components of a nonsinusoidal signal interact in the phase-lock loop.



**Robert L. Allen**

Bob Allen received his BS degree in electrical engineering from Utah State University in 1960. He worked the following summer for the *-hp-* Frequency and Time Division, and then returned to Utah State, graduating in 1961 with an MS degree in electrical engineering. In September, 1961, he joined the Frequency and Time Division full-time. He contributed to the design of the 5275A and 5243L Counters and the 107A Quartz Oscillator, and was project leader for development of the 5260A Frequency Divider and the 5240A Digital Frequency Meter. He has a patent pending and has published a paper on the method of frequency division used in the 5260A and 5240A.

Bob is a member of IEEE, Sigma Xi, Phi Kappa Phi, and Sigma Tau. By the time this article appears in print, he will have assumed new responsibilities as engineering manager of the *-hp-* Delcon Division in Mountain View, California.

Incidental FM or phase noise on the input signal and phase noise generated in the divider also affect performance, but since the curves of Fig. 5 are experimental, they include the effects of these noise signals.

Regardless of what kind of modulating signal is present, once the frequency divider locks onto an FM signal, a counter on the divider output will read the carrier frequency correctly. The modulation will be averaged out. Therefore, for FM signals, the answer to the second question stated above follows from the answer to the first, that is, if the divider can lock onto a signal, the divider output is suitable to drive a counter.

Amplitude modulation on an input signal affects the locking performance of the frequency divider as shown in Fig. 6. These curves represent experimental data for sinusoidal input signals, amplitude modulated by sinusoidal signals of frequency  $f_m$ . The ordinate is percentage amplitude modulation. Thus, the divider will lock onto an input signal at 12.4 GHz which is amplitude modulated up to 47% by a 200 kHz signal. However, if the modulating frequency  $f_m$  is 100 kHz or less, the maximum allowable AM is 30%. The increased immunity to AM at high modulation rates is caused by the rolloff in the frequency response of the main phase-lock loop. This same effect can be seen in the FM curves of Fig. 5.

Since the divider output is derived from a sampler, the output signal tends to be a lower frequency replica of the input signal. When the input signal is amplitude modulated, so is the output signal. To demonstrate this, a divider was supplied with a 1 GHz carrier, 20% amplitude modulated by a 100 kHz signal. Fig. 7 shows the corresponding output for division ratios of 100 and 1000, respectively.

If the AM causes the troughs in the envelope of the output signal to dip below the sensitivity limits of a counter connected to the output, miscounting will occur. For a counter with 100 mV sensitivity, this occurs with approximately 50% AM.

#### Acknowledgments

My associates in the electrical design of the 5260A Frequency Divider were Achille M. Bigliardi, Glenn B. DeBella, Rolf B. Hofstad, Ronald D. Lowe, Richard F. Schneider, and Ronald K. Tuttle. The electronic counter and additional circuits for the 5240A Digital Frequency Meter were designed by Ronald D. Lowe. Richard W. S. Goo served as a technician on both projects and his assistance is much appreciated. Mechanical design for both instruments was the work of Glen E. Elsea, a 10-year veteran at *-hp-*. Richard F. Schneider, who designed the zero-offset phase-lock loop, deserves special credit for his analysis and evaluation of the divider as a system and of its performance with modulated input signals. ■

— Robert L. Allen

## SPECIFICATIONS

### *-hp-* Model 5260A Frequency Divider

**RANGE:** 0.3 to 12.4 GHz  
**ACCURACY:** Retains accuracy of electronic counter.  
**INPUT SENSITIVITY:** 100 mV rms ( $-7$  dBm).  
**INPUT IMPEDANCE:** 50 ohms nominal.

Freq.	INPUT VSWR	
	Typical	Max.
0.3-8 GHz	1.2:1	1.4:1
8-10 GHz	1.4:1	1.6:1
10-12.4 GHz	1.8:1	2:1

**MAXIMUM INPUT:**  $+10$  dBm  
**LEVEL INDICATOR:** Front panel meter indicates approximate input level,  $-10$  dBm to  $+10$  dBm.  
**DIVISION RATIO:** Front panel switch selects  $\times 100$  (for use up to 1.2 GHz) or  $\times 1000$  (from 1 to 12.4 GHz) operation.  
**INPUT CONNECTOR:** Precision Type N female.  
**OPERATION:** Completely automatic once the DIVISION RATIO switch is positioned.  
**OUTPUT FREQUENCY:**  $1/100$  or  $1/1000$  of input (1 to 12.4 MHz).  
**OUTPUT IMPEDANCE:** Designed for 50 ohm load.  
**OUTPUT LEVEL:** 0 dBm, nominal.  
**REGISTRATION:** Input frequencies from 0.3 to 12.4 GHz are measured by measuring the 5260A output with an electronic counter such as the *-hp-* 5245L, 5246L or 5244L, and suitably positioning the decimal point. Readout is direct with no offset, ambiguity or arithmetic processing. See also Option 02, below.  
**PRICE:** Model 5260A Automatic Frequency Divider, \$3450.

#### OPTIONS:

01. Amphenol APC-7 Input Connector, add \$25.00.
02. Provides 5260A with circuitry such that, when used with the *-hp-* Model MO7-5245L Electronic Counter, the decimal point will be automatically positioned for readout in GHz, and the symbol 'GHz' will appear in the counter's readout. Readout suppressed when divider unlocked. Add \$175.00.

### *-hp-* Model 5240A 12.4 GHz Digital Frequency Meter FREQUENCY DIVIDER PORTION (Specifications same as 5260A)

#### LOW-FREQUENCY COUNTER PORTION

#### FREQUENCY MEASUREMENTS:

**RANGE:** 10 Hz to 12.5 MHz.  
**GATE TIME:** 0.1, 1.0 s; 10 s on special order.  
**SELF CHECK:** Counts 1 MHz for gate time chosen.

#### SIGNAL INPUT:

**SENSITIVITY:** 100 mV rms.  
**MAX. INPUT:** 2 V rms.  
**IMPEDANCE:** 1 M $\Omega$  shunted by 10 pF.

#### TIME BASE:

**FREQUENCY:** 1 MHz.  
**STABILITY:** Aging rate:  $< 2$  parts in  $10^7$ /month. As function of temperature:  $< \pm 2$  parts in  $10^6$  ( $+10^\circ\text{C}$  to  $+50^\circ\text{C}$ ),  $< \pm 20$  parts in  $10^6$  ( $0^\circ\text{C}$  to  $+65^\circ\text{C}$ ). As function of line voltage ( $\pm 10\%$ ): 1 part in  $10^7$ .  
**EXTERNAL INPUT:** 1 V rms into 1 k $\Omega$ .  
**OUTPUT:** 1 MHz, 2 V square wave into 6 k $\Omega$ .

**REMOTE RESET:** By grounding center of BNC back panel.

#### GENERAL

**ACCURACY:**  $\pm 1$  count  $\pm$  time base accuracy.

**READS IN:** MHz or GHz with positional decimal point.

**PRINTER OUTPUT:** Compatible with *-hp-* Models 562A and 5050A Digital Recorders with 1-2-4-8 BCD '1' state negative (and Option 14 for the 562A). Printers record decimal point and measurement units (562A only).

**CHASSIS CONNECTOR:** Amphenol or Cinch type 57-40500-375, *-hp-* part no. 1251-0087, 50 pin, female. Mating connector Amphenol or Cinch type 57-30500-375, *-hp-* part no. 1251-0086, 50 pin, male.

'0' STATE LEVEL:  $+8$  V

'1' STATE LEVEL: 0 V

**IMPEDANCE:** 20 k $\Omega$ , each line.

#### BCD REFERENCE LEVELS:

GROUND:  $+5$  V, 1 k $\Omega$  source.

PRINT COMMAND: 0 V to 10 V step, dc coupled.

HOLD-OFF REQUIREMENTS:  $+15$  V max.,  $+2.5$  V min.

**PRICE:** Model 5240A, \$4750.

**MANUFACTURING DIVISION:** *-hp-* Frequency and Time Division  
1501 Page Mill Road  
Palo Alto, California 94304

# Precision Measurement of Ocean Temperatures

*As ocean research becomes more sophisticated, greater precision in temperature measurement is needed*

**B**ENJAMIN FRANKLIN was able to locate and chart the Gulf Stream by hauling buckets of water on deck and measuring its temperature. Today, many northbound ships locate themselves in the Gulf Stream by towing thermometers, then take advantage of the current. This is only one of many uses for ocean temperature data.

Life in the sea, ocean currents, tidal changes, acoustic transmission, radiation absorption and heat loss are reflected by even minute ocean temperature variations. Oceanographic instruments for measuring other parameters are generally calibrated on the basis of temperature data. All of these temperature measurements require varying degrees of precision—some of them to within a millidegree C or F.

Temperature patterns are three dimensional, and both horizontal and vertical distributions influence the movement of fish. Changes of only 3 or 4 degrees C are a large change to these cold-blooded animals and have a marked effect on their metabolism and activity. In many areas, fishermen rely on temperature information to increase the size of their catch.

Temperature differences at all depths generate ocean currents, and these differences are used by oceanographers in the study of currents. The same temperature

variations influence the propagation of sound through the water, and hence influence the effectiveness of sounding, tracking and detection devices.

Because of the variety of applications of ocean temperature data, many different types of measurements are required. The most common is a measurement of the thermocline, the temperature gradient from the surface layer to the essentially isothermal deep water. Depths may range to hundreds of meters, and temperature differences may be as high as 20 degrees C. This measurement permits a prediction of sound velocity with depth and how sonar beams will deflect when directed into the water, Fig. 1.

Another important temperature gradient measurement extends over distances of one or two meters above and below the water surface. Temperature gradients of 10 millidegrees per meter or less indicate the vertical flux of heat from water to air. Most solar radiation is absorbed by the oceans of the world and converted to heat in the water. Some of this heat is transferred to the atmosphere by winds and is a primary influence on weather. These measurements are vital to the study of climate and will be used in long-range weather forecasting.

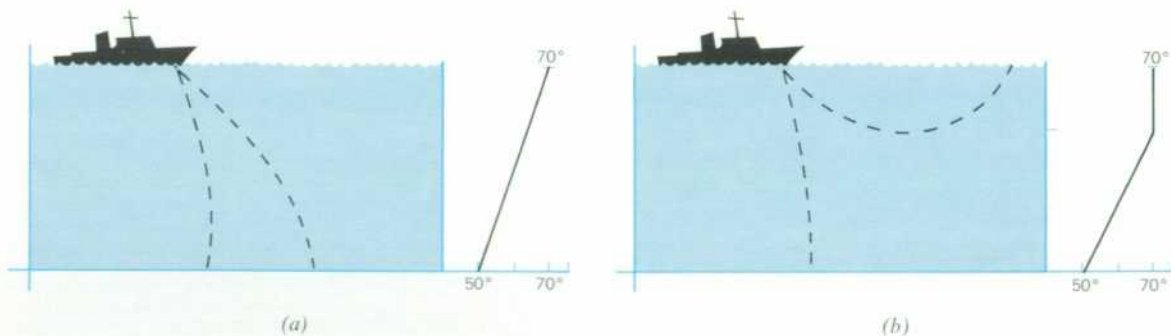
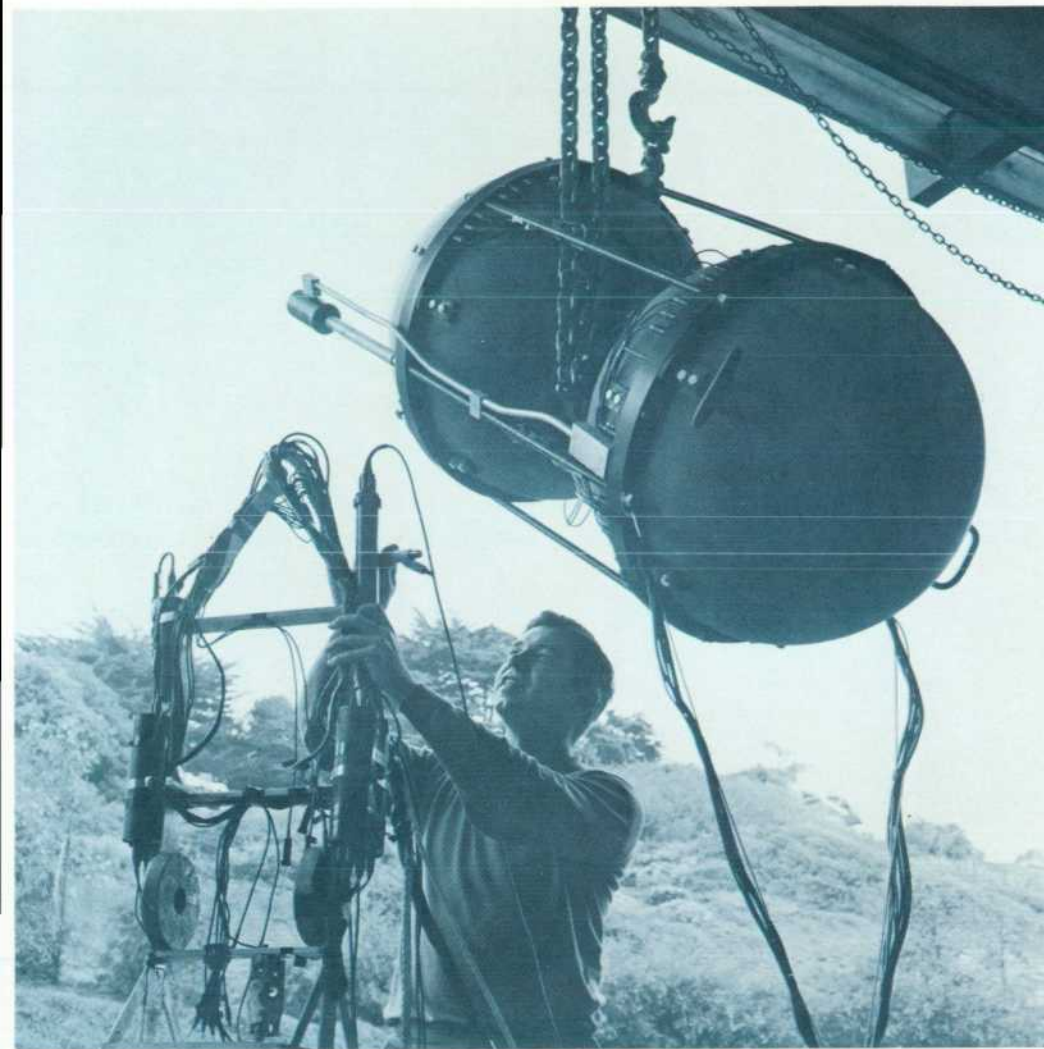


Fig. 1. Bending of a transmitted sonar beam (a) is caused by a combination of a gradual temperature change and a change in density of the water. At certain times of day, and after a storm, mixing occurs at the surface which results in a constant temperature zone. Under this condition, a sonar beam launched at an angle may return to the

surface (b). Since the beam is influenced only by a change in density and not temperature, the speed of the lower part of the wavefront is higher than the upper part causing the beam to continue to bend. An object, such as a submarine in this area may escape detection. Precise temperature measurements can detect these temperature gradients.



*Fig. 2. Temperature sensor assembly is being mounted on an instrument tripod. It can be submerged to depths over 20,000 feet and can make temperature measurements to a resolution of 1/10 millidegree.*

The measurements of salinity, depth and velocity are made with transducers which, in common with most sensors, have significant temperature coefficients which affect both their zero setting and their sensitivity. When very precise measurements are to be made, these coefficients must be determined and the necessary corrections made on the basis of the indicated 'in-situ' temperature.

An excellent example of the use of temperature measurements is in the study of tides being conducted both by the Institute of Geophysics and Planetary Physics at the Scripps Institute of Oceanography in La Jolla, California, and the Institute of Geophysics at the University of Hawaii. Until recently man was able to measure tidal changes only at the edges of an ocean's basin and on islands where he could determine tidal height with reference to the solid earth. This limited the amount of data available for a complete study of the tidal mechanism and made it difficult to locate key nodal points of the tidal oscillations.

Scripps Institute has been measuring the tide at se-

lected points in the Pacific Ocean by dropping complete instrument packages to the bottom to measure and record the changes in water pressure and temperature, Fig. 2, for periods as long as several months. The indicated pressure is a function of water height at the observation point but is also influenced by changes in water density, which can be computed with a knowledge of the temperature. The pressure sensor output which is also a function of temperature is corrected as well to determine the true tidal variations. Since the height is required to an accuracy of better than one foot and since most off-shore locations in the oceans are at depths of 10,000 to 15,000 feet, a precision of at least 0.01% is required.

#### **Instrument Design Problems**

Reliability and accuracy must be available at reasonable cost to satisfy oceanographers. Seawater corrosion, temperature variations, high pressures and high humidity contribute to severe environmental conditions that create problems common to all oceanographic instruments. For

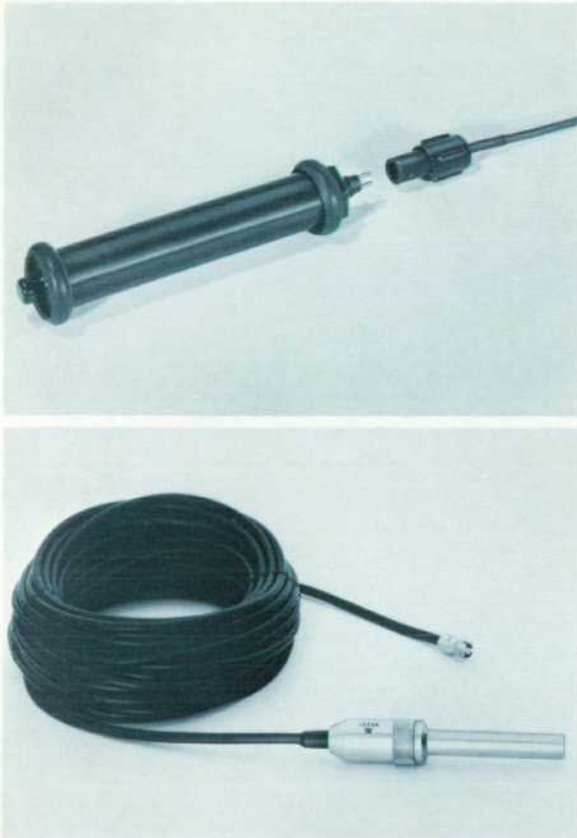


Fig. 3. A temperature sensing probe, the *-hp-* Model 2832A, top, houses the quartz crystal and all electronics in a pressure case designed specifically for measurement of ocean temperatures. At the bottom, the *-hp-* Model 2833A sensor assembly in a stainless steel case will withstand pressures to 10,000 psi and may be operated at distances up to one mile from the temperature readout.



Fig. 4. A complete quartz thermometer system, the *-hp-* Model 2801A with two temperature sensing probes. With this system, the temperature of either probe or the difference between the temperatures of the two probes can be shown on the readout.

example, it is necessary to maintain water-tight integrity under pressures as high as 15,000 to 20,000 psi. Thermometers, in addition, have the problem of self-generated heat which causes significant offsets in the order of millidegrees when located where currents are near zero. Response time, which determines how rapidly a thermometric probe can be lowered and still detect abrupt changes, is also affected by self-generated heat.

Effects of self-generated heat may be reduced by designing the probe such that the sensor is separated from the heat generating components. Choice of appropriate materials and careful mechanical design have done much to alleviate other problems.

#### Data Transmission

The oceans and their characteristics will be completely revealed only when data gathering systems provide synoptic data so that man can see the whole  $300 \times 10^6$  cubic miles simultaneously. There is a problem then, in gathering data from many sources.

Multiple strings of electrical sensors can be employed on ships, from moored buoys, and from bottom-planted systems. While the data being sensed is analog, it is usually converted to digital form for use with computing systems and digital displays. An intermediate step commonly employed to permit the telemetering of the data from sensor to system is to convert to frequency modulation immediately after the sensor to reduce inaccuracies possible in analog transmission. Then the data from individual sensors must be transmitted fairly rapidly to a central location to be reduced, correlated and plotted. However, operating systems of this type are somewhat in the future.

#### Quartz Thermometer

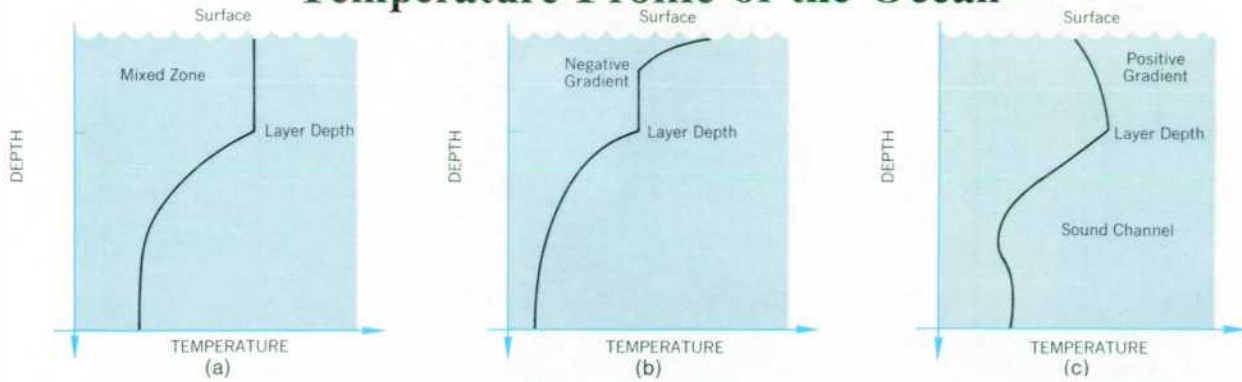
Prior to the introduction of the quartz sensor either resistance elements or thermistors were used. These may be biased with a constant current to produce a dc voltage to operate a voltage-controlled oscillator, or used in phase shift networks to influence the frequency of an RC oscillator. In either case the stability of the frequency conversion is influenced by other circuit elements in addition to the sensor itself.

The quartz temperature sensor takes advantage of the characteristic of a quartz crystal to shift its frequency of oscillation with temperature.<sup>1,2</sup> The sensor is a self-contained temperature-sensitive oscillator that requires only microwatts of power to maintain oscillation. The LC cut sensor has a precisely linear frequency-to-temperature relationship and has a sensitivity of approximately 1000 Hz per degree Centigrade.

The simplest model, Fig. 3, is the *-hp-* 2833A Tem-

1. Albert Benjaminson 'The Linear Quartz Thermometer,' *'Hewlett-Packard Journal'* Vol. 16, No. 7, Mar., 1965, p. 2.  
2. D. L. Hammond, C. A. Adams, P. Schmidt, Hewlett-Packard Co., 'A Linear Quartz Crystal Temperature Sensing Element,' presented at the 19th Annual ISA Conference, Oct. 12-15, 1964, New York. Preprint No. 11, 2-3-64.

## Temperature Profile of the Ocean



The oceans are characterized by three distinct layers: (a) an upper layer normally isothermal due to mixing by winds, a middle (thermocline) region of strong negative gradients, and a lower region of slow change extending to the bottom; (b) illustrates the 'afternoon effect' when summer heat and light winds can cause a negative gradient in the upper layer. A positive gradient (c) can also form when cool,

non-saline shelf water flows over the warm, saline Gulf Stream.

In some areas, the temperature below the thermocline decreases with depth, then increases again, forming a sound channel at the minimum temperature depth in which long sonar ranges are possible, making this characteristic very important.

perature Sensor Assembly which contains within a small stainless steel pressure case, a sensor, a solid state oscillator and an amplifier. A coaxial cable feeds dc to the unit and returns a frequency-modulated RF signal to the data acquisition instrument or system. These sensors are used singly and in arrays to provide continuous data at selected sites. Since the output frequency is determined almost entirely by the sensor itself, cable length, and temperature, or small changes in resistance or supply voltage have negligible effect on the signal. It can be transmitted 5000 feet or more without loss of accuracy. The RF signal is normally compared with a reference frequency and the difference frequency normalized and displayed in degrees C.

When very high stability is desired, the reference crystal and its companion oscillator may be placed in the same case or in duplicate cases. The AT cut reference crystal is similar to the LC cut sensor except that its temperature coefficient is only a few Hz per degree C compared with the 1000 Hz per degree C of the sensor. By mixing the signals, one benefits both from an overall calibration of the system and the advantages of transmit-

ting a smaller difference frequency to a data system or low frequency counter.

Many variations can be made of these basic combinations. Two sensor signals, Fig. 4, can be mixed to provide differential temperature readings without resorting to a reference comparison, or both absolute and differential readings can be obtained either simultaneously or sequentially. For example, in making temperature gradient measurements, one thermometer may be kept at the surface while the other is submerged. The difference may

### Cover

Showing off at 4:00 on a very windy April morning, Al Benjaminson and a crew of three sailed Al's 29-foot cutter 'Wendy Ann' 26 miles through the Golden Gate to the Farallon Islands. A continuous plot of surface temperature was made using an *-hp-* Model 2850B Quartz Thermometer mounted in a through-hull fitting. The 60-mile round trip lasted about 12 hours.

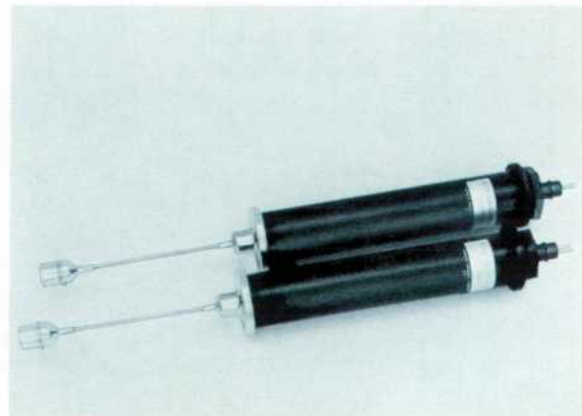


Fig. 5. Where a probe is used for precision measurements in still water, heat dissipated by the electronics in the package may heat the surrounding water, thus influencing the probe temperature. The modification shown here places the quartz crystal at some distance from the remainder of the probe and minimizes this effect.

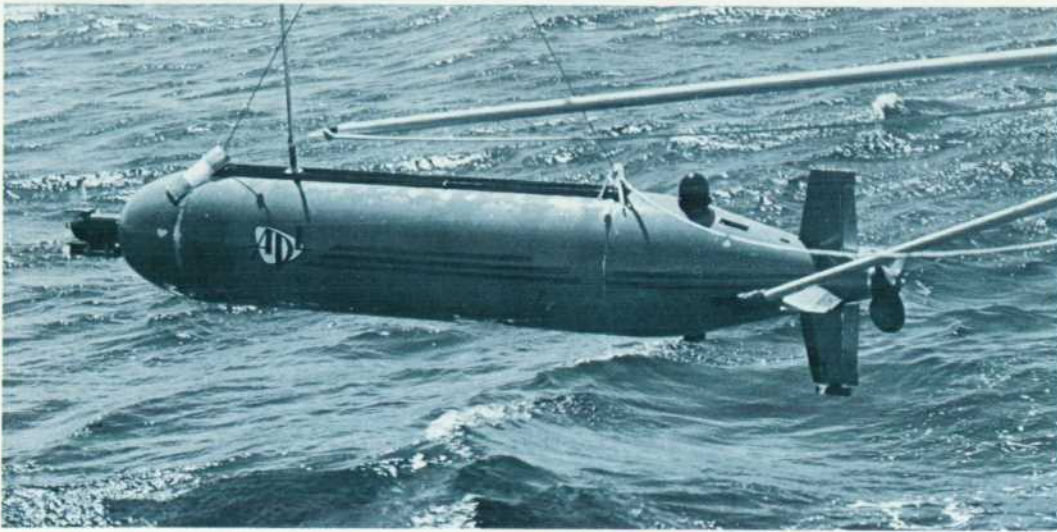


Fig. 6. Robot torpedo used by the Applied Physics Laboratory of the University of Washington for oceanographic research. A precision thermometer sensor mounted in the nose enables the vehicle to follow constant temperature lines through the water.

be read directly. Switching and scanning systems are made to read the sensors in sequence either manually or automatically. Since small changes in resistance or thermal contact voltages do not influence the accuracy, considerable freedom in switching design can be realized.

Because even the small power dissipation of a sensor assembly may create a disturbing temperature gradient around the case (as it might for extremely high accuracy measurements at the deep ocean bottom) it is practical to extend the sensor in front of the case as shown in Fig. 5, and use the larger case to provide more surface area for heat dissipation.

On a typical oceanographic vessel which may cruise to many stations and require a variety of temperature data, different types of assemblies can be used simultaneously depending upon where they are to be installed. The *-hp-*2850C probe can be installed in the condenser water intake and in the pitot log chamber, or other thru-hull fitting, usually in the deepest part of the bow. These permit continuous display, both graphical and digital, of these temperatures.

Other probes can be installed in shielded aspirators to monitor air temperatures at various levels above the sea's surface. A probe installed in a fixed station package permits vertical profiling of temperature in conjunction with salinity, pressure and other parameters of interest. A probe is frequently installed in a 'fish' and towed behind a vessel for more accurate information on sea surface temperatures. All of these probes can be connected to a central data acquisition system and scanned manually or automatically.

An interesting application of temperature sensing is made at the Applied Physics Laboratory, University of Washington, to a telechiric system (remote-controlled robot) which consists of an automatic torpedo-like 'fish,'

Fig. 6, that obeys commands sent by sonar from a surface vessel to start, stop, turn and change speed. It can be independent in vertical movement, however. The elevator mechanism is controlled either by a pressure or temperature sensor. Under these controls the 'fish' then traces the vertical pattern of an isobar (constant pressure line) or isotherm (constant temperature line), and its movements are followed by the fathometer on board the mother ship. In this way the isobar or isotherm can be completely charted, providing further information on currents, density changes and internal waves which are so vital to our growing knowledge of the sea and its parameters. ■

— Albert Benjaminson

#### Albert Benjaminson



Al Benjaminson is a graduate of the University of Adelaide, South Australia, with the degree of BEE. He had previously attended the Polytechnic Institute of Brooklyn. Before joining the Hewlett-Packard Dymec Division in 1959 he had worked as a design engineer on commercial radio products and was also a section head for military airborne electronic systems.

Since joining *-hp-*, he has been Engineering Manager of RF System Development and was responsible for the development of the phase-locked oscillator synchronizer, a microwave frequency converter and a tunable VLF receiver. In 1964 he was made engineering manager for transducer development and is responsible for quartz thermometer development.

# Improved Intermodulation Rejection in Mixers

*Intermodulation distortion, always a problem in mixer design, can be largely prevented by a careful choice of bias and power levels.*

INTERMODULATION has always been one of the most pernicious forms of spurious response in superheterodyne receivers. It is a pleasure to be able to report that this type of interference can now be vastly reduced by proper design of the mixing element of the receiver and by a proper choice of the dc operating points of the mixer diodes.

By means of the recently discovered techniques described in this article, intermodulation (IM) rejection has been improved from the 50 dB considered good in conventional mixers to over 80 dB in a single-ended hot-carrier-diode mixer and to over 100 dB in a balanced hot-carrier-diode mixer.<sup>1</sup> Moreover, this tremendous improvement in IM rejection has been obtained with little or no loss of sensitivity and little or no effect on rejection of other spurious responses. The new technique is not limited to hot carrier diodes; it can be applied to other mixing devices, and has been successfully applied in the design of a mixer using insulated-gate field-effect transistors.

## Causes of Intermodulation

Inputs to a conventional mixer are 1) a fixed-frequency local-oscillator signal and 2) the receiver input signals, which may have frequency components anywhere in the passband of the receiver input. The mixer, a square-law device, raises the sum of the input signals and the local-oscillator signal to the second power, thereby generating cross-products, some of which have frequencies that are the differences between the input frequencies and the local-oscillator frequency. These difference-frequency components are the desired outputs; other cross-products are eliminated by a bandpass intermediate-frequency (IF) amplifier.

<sup>1</sup> J. H. Lepoff and A. M. Cowley, 'Improved Intermodulation Rejection in Mixers,' IEEE Transactions on Microwave Theory and Techniques, Vol. MTT-14, No. 12, December, 1966.

Intermodulation results when harmonics of two or more incoming frequency components combine with harmonics of the local oscillator frequency to produce responses which fall within the passband of the IF amplifier. These harmonics are generated in any mixer which is not a perfect square-law device, or in other words, in any real mixer.

Spurious IM responses result when the sum of two input components and the local oscillator signal is raised to the fourth or higher power. In a diode mixer there are usually several significant higher power coefficients in the power series expansion of the diode current-vs-voltage function. This power series expansion about the dc operating point of the diode is

$$i(v) = \sum_{j=0}^{j=\infty} k_j(v-v_0)^j$$

where

$i(v)$  = diode current,  
 $v$  = diode voltage,  
 $v_0$  = diode bias voltage, or dc operating point,

$$k_j = \frac{1}{j!} \left. \frac{d^j i(v)}{dv^j} \right|_{v=v_0}$$

The coefficient  $k_2$  is the one that gives the desired square-law mixing. Terms for which  $j$  is an odd number (i.e.,  $k_1$ ,

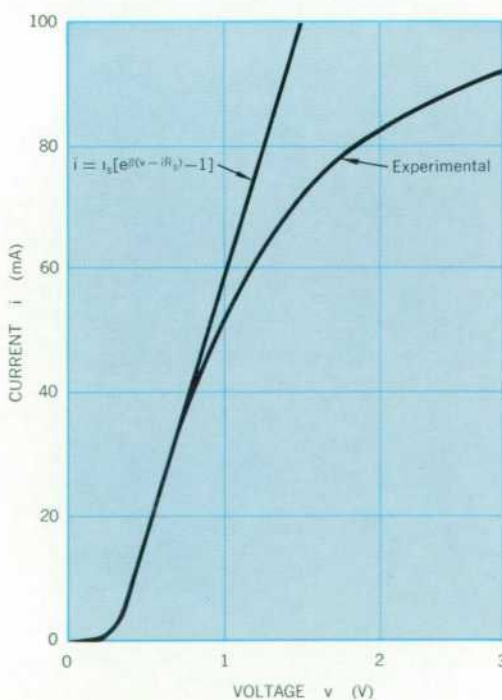


Fig. 1. Theoretical hot-carrier-diode curve and measured curve for typical hpa 2300-series diode.

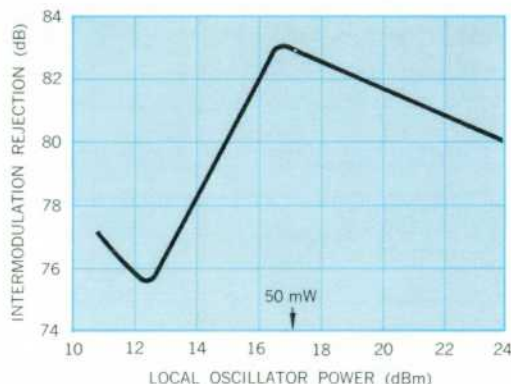


Fig. 2. Intermodulation rejection of a single-ended hot-carrier-diode mixer. Diode bias was adjusted for best IM rejection at each local-oscillator level. IM rejection can be maximized by proper selection of diode bias and LO power, as explained in text.

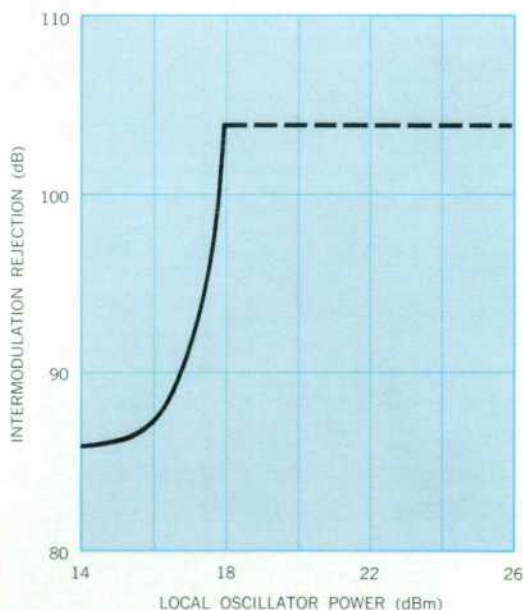


Fig. 3. IM rejection of a balanced hot-carrier-diode mixer. Diode bias voltages were adjusted for best IM rejection at each LO level. For LO power above 18 dBm, maximum desired-signal power was used, and IM was below mixer noise level.

$k_s, k_o,$  etc.) do not cause trouble because they do not produce cross-product frequencies in the IF passband. Intermodulation is caused by non-zero values of  $k_4, k_6, k_8,$  etc., in the current-vs-voltage characteristic of the diodes.

### Hot-Carrier-Diode Mixers

The current-vs-voltage characteristic of a typical hot-carrier diode is shown in Fig. 1. The top curve in Fig. 1 is calculated from the expression

$$i = i_s [e^{\beta(v - IR_s)} - 1] \quad (1)$$

where

- $i_s$  = saturation current
- $R_s$  = series resistance
- $\beta$  = constant.

Equation (1) is the usual theoretical expression for the diode current.

Also shown in Fig. 1 is an experimental curve. Values of  $\beta, i_s,$  and  $R_s$  used in calculating the theoretical curve were chosen to make the theoretical curve fit the experimental data for low currents.

Notice that for diode voltages near 1 V, the diode current drops below the theoretical curve. This means that the higher-power terms in the power series expansion of the current function are smaller at these bias levels than they are at low levels. Rejection of spurious IM responses can therefore be improved by operating the diode with a higher bias voltage than the zero bias usually used.

For still higher voltages, the diode current saturates, and the second-order term in the current function also decreases in magnitude. The second-order term is needed for mixing. Hence there is an optimum bias voltage which results in minimum spurious IM responses and still provides adequate mixing.

A second method which will result in the mixer diode's operating in the region of lower higher-power coefficients is to increase the local oscillator power. Fig. 2 shows the IM characteristics of a single-ended hot-carrier-diode mixer as a function of local-oscillator power. Bias was adjusted for optimum IM rejection at each power level. With 50 milliwatts of local-oscillator power and optimum bias, IM rejection is better than 80 dB. In this experiment, a desired signal was first applied to the mixer and the output observed. Then two spurious signals, their frequencies chosen to produce intermodulation, were applied to the mixer and their magnitudes adjusted to produce the same output as the desired signal (10 dB above the mixer noise, in this case). The two spurious signals had equal magnitudes. Intermodulation rejection was then computed as the ratio of the spurious input power (one signal) to the desired input power for the same output power.



A. Michael Cowley



Jack H. Lepoff

Mike Cowley received his BS and MS degrees in electrical engineering from the University of Notre Dame in 1959 and 1961, respectively. In 1965 he received the Ph.D. degree in electrical engineering from Stanford University, where he was employed as a research assistant in quantum electronics. Before coming to hp associates in 1965, he taught electrical engineering for a year at the University of California at Santa Barbara, and worked as a consultant in physical electronics.

Since joining hp associates, Mike has been concerned mainly with the thermal and noise properties of hot-carrier diodes. He has published six papers in the field of solid state device theory, and is a member of IEEE, Tau Beta Pi, Sigma Xi, and the American Physical Society.

After receiving his BS degree in physics from the University of New Hampshire in 1943, Jack Lepoff spent three years as a naval officer assigned to microwave component and antenna development at the Naval Research Laboratory. In 1946 he entered Columbia University as a graduate assistant in physics, and received his MA degree in 1948. From 1949 to 1965 he was associated with a number of firms and government laboratories, working on microwave components, radar, antennas, communications systems, parametric amplifiers, and tunnel diode amplifiers.

Jack joined hp associates in 1965, and assumed project responsibility for the spurious response rejection techniques project. He is now studying techniques for characterizing mixer diodes and methods of integrating semiconductor devices into microwave components.

### Balanced Mixer IM Rejection

Even better IM rejection can be obtained in a balanced mixer, for reasons which will be analyzed in the next section. Fig. 3 shows the IM characteristics of a balanced hot-carrier diode mixer with more than 100 dB of IM rejection. In measuring the data for Fig. 3, maximum input power of 5 mW was used for local-oscillator powers above +18 dBm, and the IM response was below the diode noise level. In the single-ended mixer, the slope of the IM-vs-local-oscillator-power curve is 2, whereas in the balanced mixer the slope is about 20.

### Balanced Mixer Analysis

In a balanced mixer in which the two diodes are operated at different bias voltages, some of the higher-power coefficients in the power series expansion of one diode's current function can be made to cancel the corresponding coefficients in the other diode's current function. Cancellation is the reason for the improved IM rejection of the balanced mixer of Fig. 3.

Cancellation of intermodulation is an apparent contradiction of balanced-mixer theory, which predicts summation of this response<sup>2</sup>. To show how cancellation occurs, the hypothetical diode characteristic of Fig. 4 was derived. Notice that it falls below the exponential curve just as the typical diode characteristic of Fig. 1 falls below the theoretical (exponential) curve.

<sup>2</sup> J. H. Lepoff, 'Spurious Responses in Superheterodyne Receivers,' Microwave Journal, Vol. 5, No. 6, June, 1962.

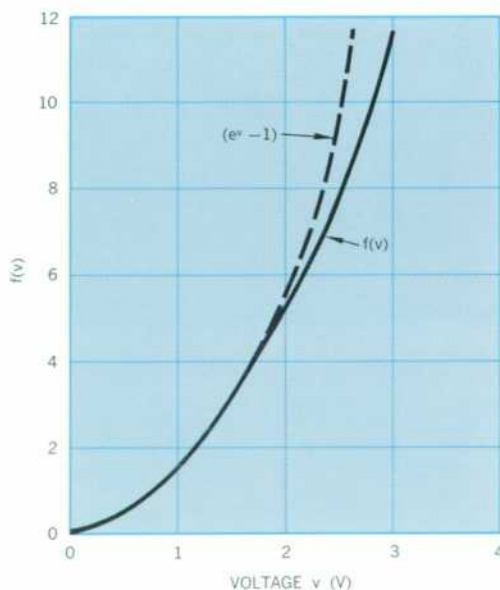


Fig. 4. Hypothetical diode characteristic used in text to illustrate cancellation of IM-producing higher-power coefficients of diode characteristics in balanced mixers.

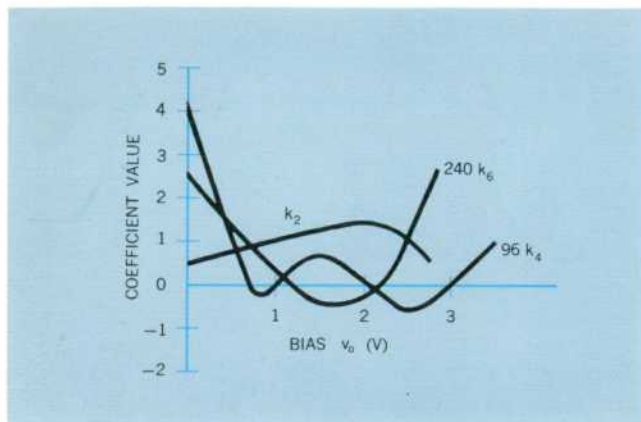


Fig. 5. Second, fourth, and sixth-power coefficients of hypothetical diode characteristic of Fig. 4. Biasing one diode of balanced mixer at 1V and the other at 2V makes  $k_4$ 's cancel and  $k_6$ 's = 0, but changes desired coefficient  $k_2$  by only a few dB.

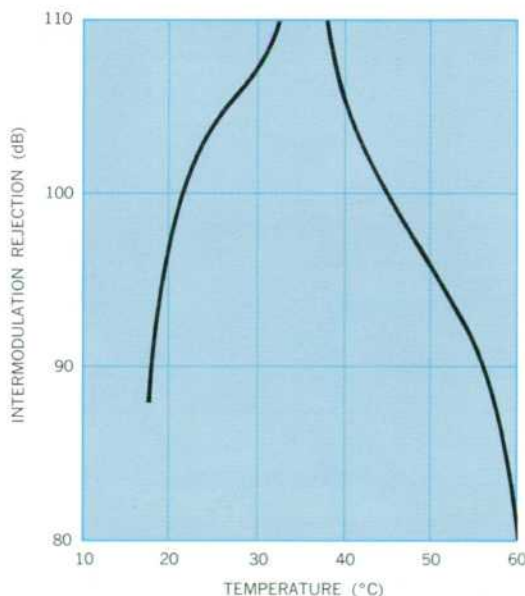


Fig. 6. Temperature dependence of IM rejection of a balanced hot-carrier-diode mixer.

In Fig. 5, the coefficients  $k_2$ ,  $k_4$ , and  $k_6$  for the hypothetical diode of Fig. 4 are plotted as functions of the bias voltage. Notice that  $k_4 = 0$  for  $v_0 = 1$  and for  $v_0 = 2$ , and  $k_6 = 0.16$  for  $v_0 = 1$  and  $-0.16$  for  $v_0 = 2$ . This means that if one diode is operated at  $v_0 = 1$  and the other at  $v_0 = 2$ , the IM response in the mixer output due to the fourth and sixth power terms will be zero. These terms are the most serious causes of intermodulation in conventional mixers.

Departure of the diode characteristics from exponential at high bias voltages, as shown in both Fig. 1 and Fig. 5, is necessary for cancellation or reduction of IM-producing higher-power terms. Pure exponential behavior will not produce any benefit from high bias, high local-oscillator power, or unbalanced bias. However, measured characteristics of hot-carrier diodes, point-contact diodes, and other mixing devices do depart from exponential at high bias voltages.

#### Sensitivity

The techniques described here for reducing IM responses would be of little value if they caused an excessive loss of mixer sensitivity. Fortunately, they do not. For a given local oscillator power and desired-signal input power, the desired response is proportional to the coefficient  $k_2$ . This coefficient for the fictitious diode of Fig. 4 is also plotted in Fig. 5. Note that  $k_2$  does not change by more than a factor of three for  $0 < v_0 < 2.5$ , which means that the sensitivity of a mixer using these diodes would not be changed by more than a few dB by adjustment of the bias for maximum IM rejection.

#### Effects of Temperature

Fig. 6 shows the temperature sensitivity of the IM characteristic of a balanced hot-carrier-diode mixer. Rejection remains high for a 25  $^{\circ}$ C range. Operation over wider temperature ranges may be possible if thermistors are used in the bias circuit.

#### Acknowledgment

The authors are grateful to Stewart Krakauer for valuable suggestions during the work described in this article. ■ — A. Michael Cowley and Jack H. Lepoff